

Article

Quality Assessments of Shallow Groundwaters for Drinking and Irrigation Purposes: Insights from a Case Study (Jinta Basin, Heihe Drainage Area, Northwest China)

Jianguo Feng ¹, Hao Sun ¹, Minghao He ², Zongjun Gao ^{1,*}, Jiutan Liu ³, Xi Wu ⁴ and Yonghui An ⁴

¹ College of Earth Science and Engineering, Shandong University of Science and Technology, Qingdao 266590, China; fengjianguo20316@sohu.com (J.F.); shsdust@126.com (H.S.)

² Sixth Team of Jilin Nonferrous Metals Geological Exploration Bureau, Tonghua 134002, China; hmhsdust@126.com

³ College of Energy and Mining Engineering, Shandong University of Science and Technology, Qingdao 266590, China; ljtsdust@126.com

⁴ Center for Hydrogeology and Environmental Geology Survey, China Geological Survey, Baoding 071051, China; wuxi1911@163.com (X.W.); anyonghui@126.com (Y.A.)

* Correspondence: zongjungao1964@163.com

Received: 26 July 2020; Accepted: 24 September 2020; Published: 27 September 2020



Abstract: This study aimed to determine the hydrochemical characteristics and hydrogeochemical processes of shallow groundwater in the Jinta Basin, northwest China, and to evaluate the suitability of groundwater quality for drinking water and agricultural irrigation. A systematic hydrogeological survey was conducted in the study area from May 2017 to October 2018, during which 123 representative samples of groundwater were selected for analysis of chemical parameters and determination of the water quality index. The results showed that the pH of groundwater in the study area was weakly alkaline and ranged between 7.21–8.93. Dominant cations were Mg^{2+} and Na^+ and the dominant anion was SO_4^{2-} . Along the groundwater flow from the southwest to northeast, the dominant groundwater chemistry type in the recharge area was $Mg-HCO_3 \cdot SO_4$. After the transition of the groundwater types in the runoff area to $Mg-SO_4 \cdot HCO_3$ and $Mg \cdot Na-SO_4$, the groundwater type in the discharge area evolved into $Na \cdot Mg-SO_4 \cdot Cl$. The major factors driving the evolution of groundwater chemical types in the Jinta Basin were found to be rock weathering, evaporation and precipitation. The chemical components of groundwater mainly originated from the dissolution of silicate rock and evaporative concentration of salt under water-rock interaction, whereas the dissolution of carbonate had little influence. The quality of drinking water was divided into five groups, and 39.84% of samples fell within the high and good quality groups. The quality of agricultural irrigation water was divided into different grades according to different methods.

Keywords: groundwater; hydrochemical characteristics; water quality evaluation; Jinta Basin

1. Introduction

Exploitation of groundwater has expanded greatly in China in recent decades. Rapid population growth and economic development has led to the extraction of groundwater for drinking, irrigation and industrial purposes. Over-exploitation of groundwater can affect both the quantity and quality of groundwater, and there has been a realization by the government and water management agencies in China that the quality of groundwater is just as important as quantity. The northwest region of China

is an arid/semi-arid region situated in the hinterland of Eurasia, and is characterized by a dry climate, scarce rainfall and relatively limited runoff of inland rivers. Groundwater resources play an important role in sustaining life and human development in this region. The ecological environment of this region is also relatively fragile due to considerable desertification and scarce vegetation. Sustainable use of groundwater in this region is vital for the maintenance of the ecological balance and ensuring harmonious development between man and nature [1–3]. Groundwater in this region is impacted by both natural and anthropogenic effects, including local climate, geology, hydrogeology and mode of development and utilization.

The Jinta Basin is located in the middle and lower parts of the Hexi Corridor in the northwestern part of Gansu Province. The basin falls into a continental temperate arid climate area characterized by scarce precipitation and strong evaporation and forms the middle and lower reaches of the Heihe River Basin [4]. Water for domestic use and agricultural irrigation in this area is mainly sourced through groundwater exploitation. The water table in the basin has experienced continual decline in recent years with an increase in the number of wells extracting groundwater for agricultural irrigation, which has had a serious impact on the ecological environment of the region [5]. The changes in groundwater resources through over-exploitation, a changing climate and increasing human activities will result in a change in groundwater quality. The deterioration of water quality will exacerbate water deficits and endanger the natural environment. An analysis of the characteristics of the major ionic components of groundwater can reveal the underlying processes controlling the chemical composition of groundwater. At the same time, the characterization of the groundwater quality in relation to drinking water and agricultural irrigation water quality standards can act as an important reference for the rational utilization of water resources and the protection of the ecological environment.

The majority of previous studies of groundwater hydrochemistry in the Jinta Basin concentrated on small subcatchments of the basin, and there have been few studies of groundwater hydrochemistry across the entire basin. Cui et al. [6] studied spatial and temporal variations in land-use type in the Jiuquan-Jinta Basin in 2014 with the aim of evaluating the value of ecosystem services. Li [7] studied the water resources carrying capacity of the Jinta Basin through the use of a system dynamics model. Ma [8] focused on the major anions of groundwater in the Heihe River Basin, and used correlation analysis methods such as the ion ratio method, piper diagrams and the chloralkaline index to analyze the hydrochemical characteristics of groundwater and the influence of the exchange effect. Jianlong simulated the hydrogeochemical evolution of groundwater using the PHREEQC software [9]. The studies mentioned above have not evaluated the groundwater quality of the Jinta Basin, which is of value for guiding the development and utilization of groundwater in the basin. The water quality index (WQI) has been widely used in recent years for the characterization of groundwater quality [10]. For example, Papazotset et al. [11] use the WQI to examine the suitability of groundwater in the Marathon Basin, northeast Attica, Greece, for drinking water and irrigation.

The current study characterises the hydrochemical characteristics and water quality of shallow groundwater in the Jinta Basin using the most recent observed data with the aims of identifying the underlying geochemical processes controlling the concentrations and spatial variability of various groundwater hydrogeochemical parameters and assessing the suitability of groundwater resources for drinking water and agricultural irrigation.

2. Study Area

The Jinta Basin has a surface area of ~ 4974 km², is situated between Mazong Mountain and Jinta Nanshan and is connected to the Huahai Basin in the west and Badain Jaran desert in the east. The Jinta Basin is surrounded by mountains in the north and south (Figure 1). The central part of the basin is low and flat and the terrain is slightly inclined. The Jinta Mountain forms the southern boundary of the basin and has an altitude of ~ 1420 m. The maximum height difference within the Jinta basin is less than 200 m. A near east–west fault has developed in the basin and forms part of the eastern extension of the Altun fault zone. This fault is characterized by a sinistral strike slip and forms the boundary

between the Jiuquan East Basin and the Jinta Basin. The Mazong Mountain is situated in the northern part of the basin and has a maximum elevation of 2583 m and a relative height difference ranging between 45–1338 m. The Mazong Mountain was formed by the convergence and compression of the Tarim, China–Korea and Mongolia plates.

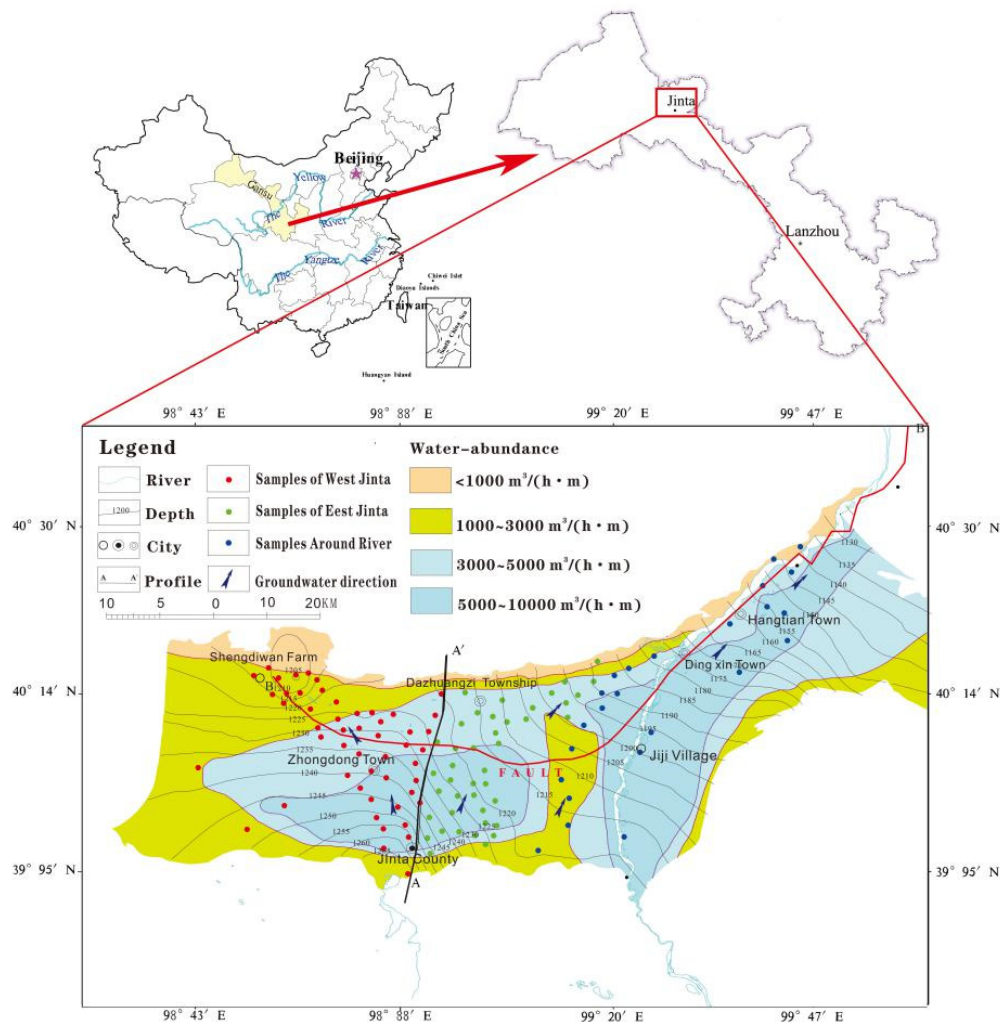


Figure 1. Map of the Jinta Basin within China and the locations of groundwater sampling points.

According to meteorological data collated by the Jinta County Meteorological Bureau for 1989 to 2017, the average, lowest and highest temperatures of the Jinta Basin are 8.9–29.6 °C and 39.5 °C, respectively. The annual precipitation in the basin is mostly concentrated during June to September, and the basin has an annual average rainfall and potential evaporation (water surface evaporation) of 56.3 mm and 2538.6 mm, respectively. Groundwater resources account for ~21% of total water resources in the region and the current groundwater management policies allow groundwater exploitation [7,9]. The distribution of groundwater in the Jinta Basin shows clear regularity and zoning. From south to north and from west to east, there is a decrease in groundwater depth, the particles of the aquifer changes from coarse to fine, and the permeability and water yield of the aquifer increase. The quaternary system in the southern part of the Jinta Basin has a thickness exceeding 200 m and an aquifer lithology that can be described as sand gravel, medium coarse sand and fine sand with a good water yield. The thickness of the quaternary system in front of the Mazong mountain in the north is less than 50 m, and the aquifer lithology of this region can be described as fine and medium sand with a general water yield (Figure 2).

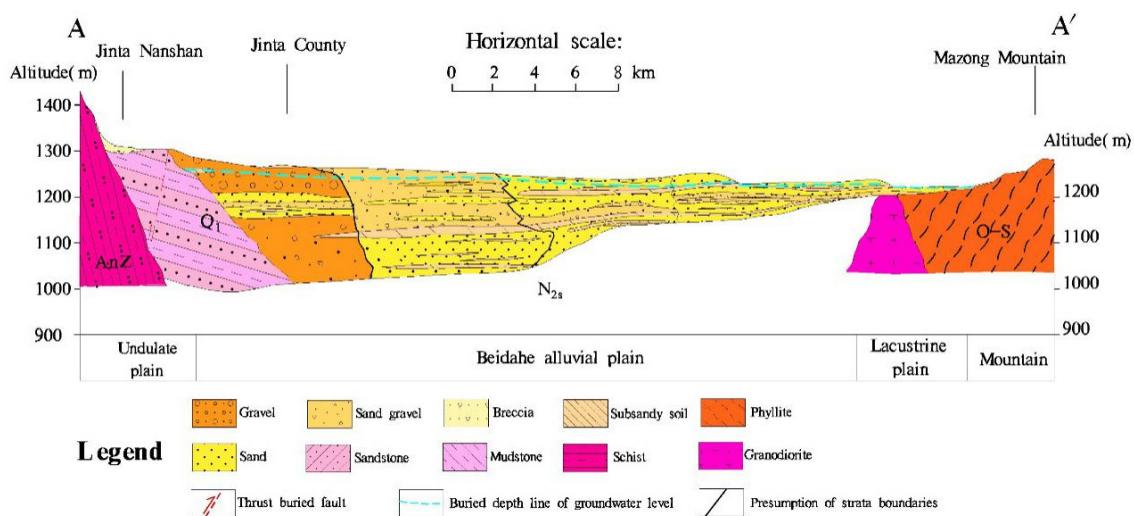


Figure 2. A–A' Hydrogeological profile of the Jinta Basin, China.

3. Methods and Materials

3.1. Sampling and Analysis

The hydrochemical data analyzed in the present study originated from the “1:50,000 hydrogeological survey of the Heihe River Basin in Hexi Corridor” project that was conducted by the Center for Hydrogeology and Environmental Geology Survey of China Geological Survey Bureau. During this project, groundwater wells in the Jinta Basin were systematically investigated, and 123 representative groundwater samples were collected from a depth of between 3.00–163.70 m from May 2017 to October 2018. The sample sites are divided into three parts: west Jiuquan, with 51 samples; east Jiuquan, with 43 samples; the samples around Hei River have 28. The global positioning system (GPS) was used to identify the coordinates and elevation of each sampling point.

Samples were collected from both production and pressure wells. Prior to sampling, sampling bottles were sterilized and rinsed in distilled water. During sampling, the groundwater pump was run for more than 10 min and the sample bottle was rinsed at least three times before a sample was taken. The chemical constituents of the collected groundwater samples were determined by laboratories at the Institute of Hydrogeology and Engineering Geology of the Gansu Provincial Bureau of Geology and Mineral Resources. Temperature, total dissolved solids (TDS), pH of the groundwater samples were determined using a water quality multi-meter (HACH). The groundwater concentrations of Ca^{2+} , Mg^{2+} , Na^+ and K^+ were determined by inductively coupled plasma (ICP) emission spectrometry. The groundwater concentrations of Cl^- , SO_4^{2-} and NO_3^- were determined by ion chromatography, whereas HCO_3^- was determined by titration. The test methods used were strictly in accordance with standard groundwater quality testing methods (DZ/T0064-93).

The routine water quality indicators were selected for further analysis, including pH, TDS, K^+ , Na^+ , Ca^{2+} , Mg^{2+} , Cl^- , SO_4^{2-} , HCO_3^- and NO_3^- . Piper three-line maps, statistical analysis in the SPSS software package, correlation analysis, the Gibbs model and end-element maps of ion ratios were used to study the hydrochemical characteristics of shallow groundwater in the Jinta Basin and the underlying processes. Ion balance error calculated to assess the accuracy of the analysis showed that all determinations were within $\pm 5\%$.

3.2. Analysis of Hydrogeochemical Processes

Piper diagrams have been widely used in the study of groundwater types and for the analysis of hydrochemical processes controlling groundwater chemical composition. Gibbs plots can be used to

determine the major mechanisms controlling groundwater chemistry, such as rock–water interactions, dominance by either precipitation or evaporation and dominant water chemistry. The use of ratio graphs of ions is an effective graphical method for determining the origins of solutes and identifying important hydrogeochemical processes.

3.3. Method Used in the Assessment of Groundwater Quality

3.3.1. Drinking Water Quality Assessment

The water quality index (WQI) is a simple and effective approach for determining the overall quality of groundwater and its suitability for drinking purposes as this index reflects the influences of a number of different water quality parameters on overall groundwater quality [12,13]. The WQI index was selected in the current study to evaluate the drinking water quality of the groundwater samples according to standards of the World Health Organization (WHO, 2004). Firstly, weights (w_i) were assigned to ten selected parameters in the relative importance of $\text{pH} > \text{TDS} > \text{Ca}^{2+} > \text{Mg}^{2+} > \text{Na}^+ > \text{K}^+ > \text{HCO}_3^- > \text{Cl}^- > \text{SO}_4^{2-} > \text{NO}_3^-$ (Table 1) [14,15]. The WQI was then calculated according to Equations (1)–(4).

$$Wi = \frac{wi}{\sum_{i=1}^n wi} \quad (1)$$

Table 1. The weight (w_i) and relative weight (Wi) of each chemical parameter calculated based on the standard values reported by the World Health Organization (WHO, 2004).

Parameter	WHO Standards (mg L ⁻¹ , Except pH)	Weight (w_i)	Relative Weights (Wi)
pH	8.5	3	0.083
TDS	500	5	0.139
Ca ²⁺	75	3	0.083
Mg ²⁺	50	3	0.083
Na ⁺	200	4	0.111
K ⁺	12	2	0.056
HCO ₃ ⁻	120	1	0.028
Cl ⁻	250	5	0.139
SO ₄ ²⁻	250	5	0.139
NO ₃ ⁻	11	5	0.139
Σ	–	–	1

Abbreviations: TDS: total dissolved solids.

In Equation (1), Wi is the relative weight, w_i is the weight of each parameter and n is the total number of parameters.

$$qi = \frac{Ci}{Si} \times 100 \quad (2)$$

In Equation (2), qi is the quality rating, Ci is the concentration of each chemical parameter in each sample (mg L⁻¹, except pH) and Si is the standard limit for each chemical parameter (mg L⁻¹, except pH) according to the WHO guidelines for 2004.

$$Sli = Wi \times qi \quad (3)$$

$$WQI = \sum_{i=1}^n Sli \quad (4)$$

In Equation (3) and Equation (4), Sli is the sub-index of the parameter, qi is the rating based on the concentration of the parameter and n is the total number of parameters. The classification of groundwater quality was showed by Table 2:

Table 2. Classification of groundwater quality on the basis of the water quality index (WQI).

Range	Type of Groundwater	Number of Samples	Percentage of Samples (%)
50	Excellent water	4	3.25
50–99.99	Good water	45	36.59
100–199.99	Poor water	30	24.39
200–299.99	Very poor water	19	15.45
≥300	Unsuitable for drinking purposes	25	20.32

3.3.2. Assessment of the Quality of Groundwater Samples for Use in Agricultural Irrigation

The suitability of groundwater for irrigation mainly depends on the concentrations of total salinity and sodium. The quality and suitability of groundwater for use in agricultural irrigation was assessed in the current study by certain commonly used indices, including the sodium adsorption ratio (SAR), sodium percentage (%Na), Kelley's ratio (KR) and permeability index (PI).

Sodium Adsorption Ratio (SAR)

The sodium adsorption ratio (SAR) is an important parameter for determining the suitability of groundwater for irrigation purposes [16,17].

The SAR values were calculated using Equation (5) [18]:

$$\text{SAR} = \frac{\text{Na}^+}{\sqrt{\frac{\text{Ca}^{2+} + \text{Mg}^{2+}}{2}}} \quad (5)$$

In Equation (5), all ionic concentrations are expressed in meq L^{-1} .

Sodium Percentage (Na%)

Sodium percent (Na%) is considered an important parameter for the assessment of groundwater suitability for irrigation water, as sodium decreases the soil fertility [19]. Equation (6) was used to calculate Na% [10]:

$$\text{Na}\% = \frac{\text{Na}^+ + \text{K}^+}{\text{Ca}^{2+} + \text{Mg}^{2+} + \text{Na}^+ + \text{K}^+} \times 100 \quad (6)$$

In Equation (6), all ionic concentrations are expressed in meq L^{-1} .

Kelley's Ratio (KR)

Equation (7) was used to calculate the KR parameter [20]:

$$\text{KR} = \frac{\text{Na}^+}{\text{Ca}^{2+} + \text{Mg}^{2+}} \quad (7)$$

In Equation (7), all ionic concentrations are expressed in meq L^{-1} .

Permeability Index (PI)

The permeability of soil is influenced by sodium, calcium, magnesium and bicarbonate in soil as well as by the long-term use of irrigation water. Doneen established the permeability index (PI) for use as an indicator of irrigation water quality [21,22].

Equation (8) was used to calculate the PI parameter:

$$\text{PI} = \frac{\text{Na}^+ + (\text{HCO}_3)^{\frac{1}{2}}}{\text{Ca}^{2+} + \text{Mg}^{2+} + \text{Na}^+} \times 100 \quad (8)$$

In Equation (8), all ionic concentrations are expressed in meq L^{-1} .

4. Results and Discussion

4.1. Hydrochemical Composition of Groundwater Samples

4.1.1. Characteristics of Major Ions

Table 3 shows a summary of the hydrochemistry of the 123 shallow groundwater samples collected from the Jinta Basin. The results show that groundwater pH ranges between 7.19–8.91 with an average of 7.85 and a coefficient of variation of below 0.05. This result indicates that groundwater in the study area is mainly weak alkaline and that there is little spatiotemporal variation in pH of groundwater in the study area. TDS ranged between 339–11,513 with an average of 1816.68. The rank of cations in groundwater according to abundance was $\text{Na}^+ > \text{Mg}^{2+} > \text{Ca}^{2+} > \text{K}^+$ whereas that of the anions was $\text{SO}_4^{2-} > \text{HCO}_3^- > \text{Cl}^- > \text{NO}_3^-$. The coefficient of variation is the quotient of standard deviation and the corresponding average value, and is typically used to characterize the stability of variables [23]. The results showed that the coefficient of variation of each ion concentration ranged between 0.46–1.56, thereby indicating that the contents of these ions in pore water of the Jinta Basin showed considerable spatial variation and were sensitive to driving factors.

Table 3. Statistical summary of the hydrochemistry of groundwater samples collected from the Jinta Basin, China.

Parameters	pH	TDS	Ca^{2+}	Mg^{2+}	Na^+	K^+	HCO_3^-	Cl^-	SO_4^{2-}	NO_3^-
Maximum	8.91	11,513.00	550.90	1124.00	1468.00	46.60	907.90	1592.00	6519.00	127.34
Minimum	7.19	339.00	22.50	14.50	29.40	3.60	68.30	19.10	96.50	0.50
Average	7.85	1864.67	109.18	183.00	227.99	12.97	295.02	240.43	915.92	10.75
Standard Deviation	0.39	1816.02	89.48	176.06	255.90	9.20	136.04	286.76	1017.32	16.75
Coefficient of Variation	0.05	0.97	0.82	0.96	1.12	0.71	0.46	1.19	1.11	1.56

4.1.2. Correlation Analysis

Correlation analysis of groundwater hydrochemistry can be used to identify certain correlations between the dominant ions in groundwater [24]. A correlation analysis of chemical indices was conducted using the SPSS software, with the results shown in Table 4. There were relatively significant correlations between TDS and Ca^{2+} , Mg^{2+} , K^+ and SO_4^{2-} , with correlation coefficients of 0.874, 0.757, 0.855, 0.238 and 0.973, respectively. The strong relationships between TDS and Ca^{2+} , Mg^{2+} , K^+ and SO_4^{2-} indicated that weathering and dissolution of sulfate rock may be important processes in determining groundwater types. The correlations between HCO_3^- and K^+ and between HCO_3^- and Ca^{2+} obtained correlation coefficients of 0.895 and 0.929, respectively, indicating a certain relationship between HCO_3^- and these two ions, possibly due to the weathering dissolution of carbonate rocks. A strong correlation was obtained between Cl^- and Na^+ , with a correlation coefficient of 0.946, indicating a strong relationship between Cl^- and Na^+ , possibly due to the dissolution and evaporation of rock salt. There was also a strong correlation between SO_4^{2-} and Mg^{2+} with a correlation coefficient of 0.984, thereby indicating that Mg^{2+} may be derived from the dissolution of magnesium-bearing sulfate rocks.

It is worth stressing that an assumption of high correlations (>0.9) among various indices being simply due to weathering of a certain rock would mean that other drivers have very weak influence on these indices. This is obviously not a rigorous assumption; therefore, it was necessary to further analyze the drivers of hydrochemical types.

4.1.3. Factor Analysis

Factor analysis was used to analyze the relationships between ions. The results of factor analysis were used to reveal the processes driving spatiotemporal variations in some major ions in the Jinta Basin. The groundwater data collected from the Jinta Basin were standardized and analyzed using the

Kaiser–Meyer–Olkin (KMO) test and the Bartlett spherical test. The KMO and Bartlett measures were 0.647 and 0, respectively, thereby indicating that the data were suitable for factor analysis [25,26].

Table 4. The correlation coefficient matrix between the various chemical indicators within groundwater samples collected from the Jinta Basin, China.

Index	pH	TDS	Ca ²⁺	Mg ²⁺	Na ⁺	K ⁺	HCO ₃ ⁻	Cl ⁻	SO ₄ ²⁻	NO ₃ ⁻
pH	1									
TDS	-0.266	1								
Ca ²⁺	-0.297	0.952	1							
Mg ²⁺	-0.289	0.973	0.917	1						
Na ⁺	<u>-0.214</u>	0.959	0.895	0.874	1					
K ⁺	-0.401	0.727	0.671	0.757	0.644	1				
HCO ₃ ⁻	-0.593	0.365	0.353	0.415	0.298	0.565	1			
Cl ⁻	-0.179	0.936	0.917	0.855	0.963	0.564	<u>0.221</u>	1		
SO ₄ ²⁻	-0.247	0.992	0.935	0.984	0.929	0.733	0.330	0.895	1	
NO ₃ ⁻	-0.360	0.258	0.272	0.238	0.264	0.377	0.542	<u>0.221</u>	<u>0.208</u>	1

Underlined entries indicate very significant correlations at the 0.05 level (two-tailed); shaded entries indicate correlations significant at the 0.01 level (two-tailed).

According to the screening requirement of an eigenvalue greater than one, the cumulative variance contribution rates of the two major factors extracted in the present study reached 87.501%. As shown in Table 5, the contribution rate of the first factor was 65.925% and was closely related to SO₄²⁻, Cl⁻, Na⁺, Mg²⁺, Ca²⁺ and K⁺, which can be interpreted as the processes of weathering and dissolution of silicate and evaporite rocks. The contribution rate of the second factor was 17.466% and it showed strong correlations with HCO₃⁻ and NO₃⁻. Since the major source of NO₃⁻ in the study area is the use of nitrogen fertilizer [27], the processes linked to the second factor can be interpreted to be agricultural production activities and the dissolution of the carbonate (Table 5).

Table 5. Rotated component matrix.

Index	Factor	
	First Factor	Second Factor
TDS	0.98	0.14
pH	-0.39	0.69
Ca ²⁺	0.95	-0.11
Mg ²⁺	0.97	-0.12
Na ⁺	0.94	-0.16
K ⁺	0.84	0.18
SO ₄ ²⁻	0.97	-0.19
Cl ⁻	0.94	-0.20
HCO ₃ ⁻	0.57	0.67
NO ₃ ⁻	0.26	0.86
Characteristic value	6.59	1.747
Contribution rate (%)	65.93	17.466
Cumulative contribution (%)	65.93	83.391

4.2. Analysis of Hydrochemical Genesis Types

4.2.1. Analysis of Hydrochemical Characteristics

The Piper diagram is an important method for analyzing changes in the groundwater composition of major ions and is also a method of visualizing hydrochemical characteristics [28]. The Aq.QA software was used to construct Piper three-line diagrams for pore water of the study area (Figure 3). The majority of samples were concentrated in the upper right corner of the cationic triangle diagram, except for the relatively dispersed distribution of individual water samples. The majority of Mg²⁺ equivalent percentages among the 123 samples exceeded 40%, indicating that Mg²⁺ was a major cation

in pore water. Water samples were more dispersed in the anionic triangle diagram, although it was evident that SO_4^{2-} was a major anion. Comprehensive analysis showed the major chemical types of pore water in the study area to be Mg-SO_4 , Mg-Na-SO_4 , $\text{Na-Mg-SO}_4\cdot\text{HCO}_3$ and $\text{Na-Mg-SO}_4\cdot\text{Cl}$. In the three runoff areas, HCO_3^- decreased along the groundwater flow direction.

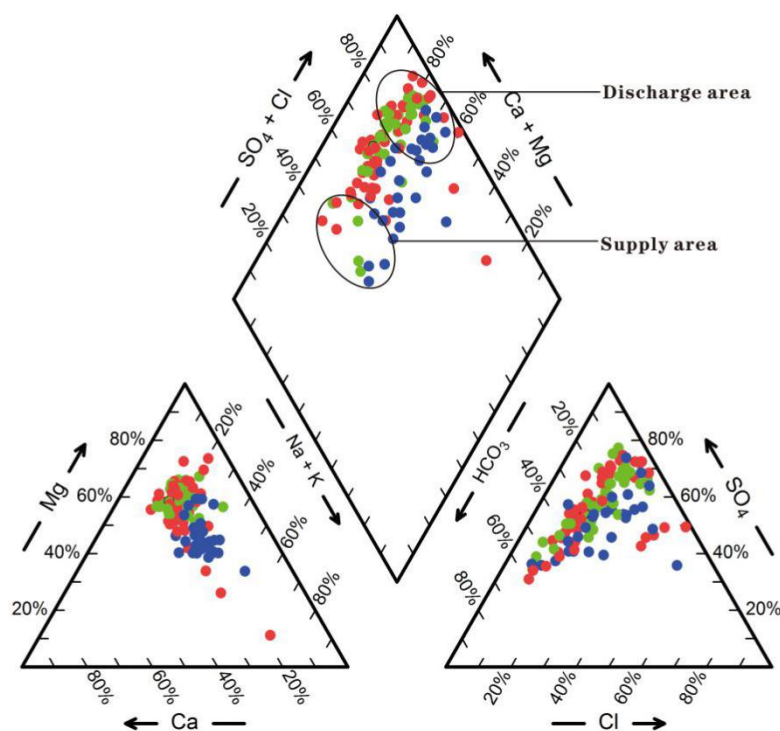


Figure 3. Piper three-line diagram of shallow groundwater in the Jinta Basin, China.

4.2.2. Water–Rock Model Analysis

The Gibbs plot is an important method used to analyze the major factors controlling the evolution of groundwater chemical types, such as evaporation crystallization, rock weathering and atmospheric precipitation [29]. The range of TDS in groundwater in the study area was 339–11513, with the ratios of cation concentrations $\text{Na}^+ / (\text{Na}^+ + \text{Ca}^{2+})$ being 0.33–0.88, whereas the ratio of anion concentrations $\text{Cl}^- / (\text{Cl}^- + \text{HCO}_3^-)$ was 0.08–0.94. As shown in Figure 4, weathering and evaporative crystallization of rocks were the major factors identified in the $\text{Cl}^- / (\text{Cl}^- + \text{HCO}_3^-)$ diagram. This result indicated that evaporative crystallization of $\text{Na}^+ / (\text{Na}^+ + \text{Ca}^{2+})$ was the major factor influencing anion compositions. The effect of atmospheric precipitation on the chemical composition of groundwater in the study area is extremely weak since the study area is located in an arid inland area. Continuous leaching of groundwater in the basin has resulted in the chemical components in groundwater mainly originating from mineral dissolution via water–rock interactions and in the TDS concentrations being low. The aquifer gradually changed from receiving replenishment to being a net discharger of flow along the direction of groundwater runoff, and aquifer soil particles become finer, groundwater flowed more slowly, evaporation increased and the concentrations of Na^+ and Cl^- increased.

Figure 5 shows end-member diagrams constructed using hydrochemistry data from the 123 groundwater samples in the study area. These diagrams were further analyzed to review the sources of chemical ion components in groundwater [30]. Figure 5 shows that the hydrochemical composition of each sampling point ranged between the silicate rock and evaporite rock area, with a larger number of samples occurring in the silicate rock area. This result demonstrates that the weathering of silicate rock and evaporite are the major processes controlling groundwater hydrochemistry in the study area, which was consistent with the results of the Gibbs diagram.

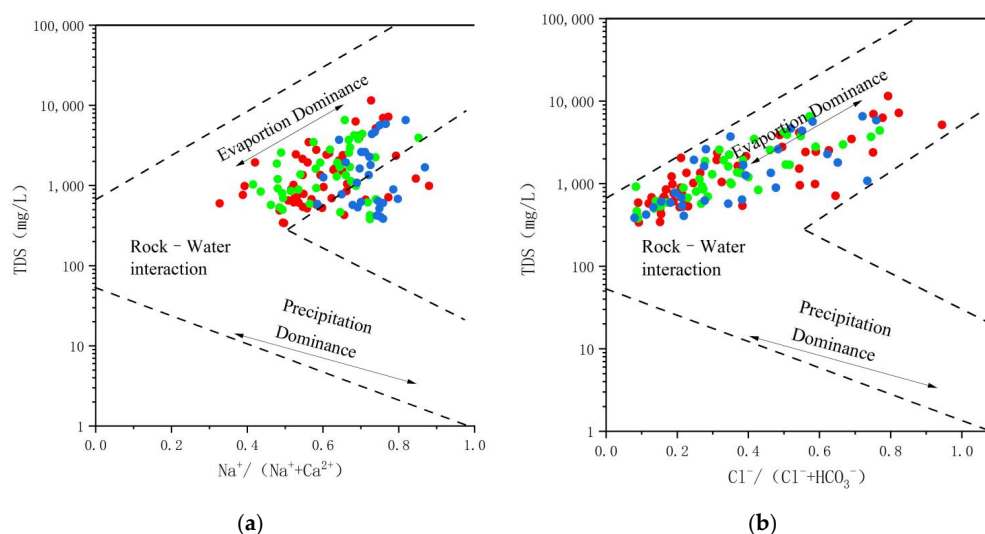


Figure 4. Gibbs diagram of groundwater samples collected from the Jinta Basin, China. (a): TDS versus $\text{Na}^+ / (\text{Na}^+ + \text{Ca}^{2+})$, (b): TDS versus $\text{Cl}^- / (\text{Cl}^- + \text{HCO}_3^-)$.

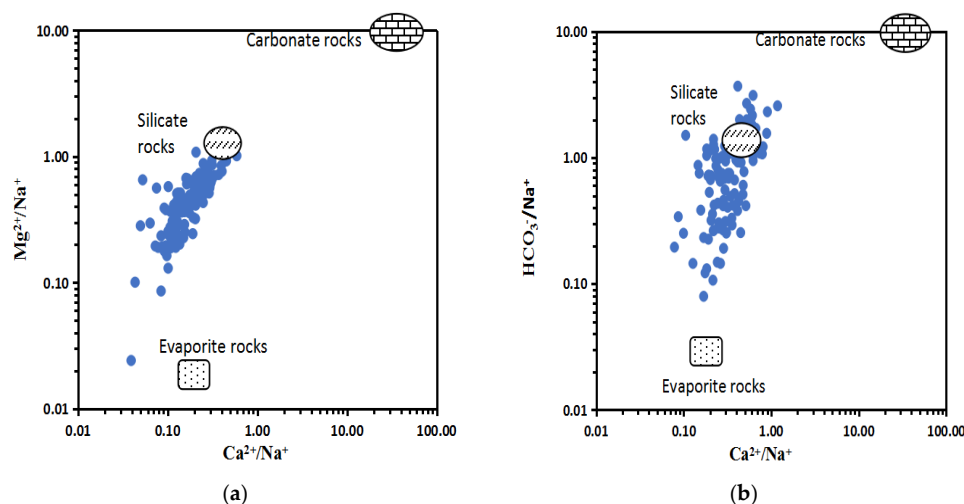


Figure 5. End-member diagrams for groundwater samples collected from the Jinta Basin, China. (a): $\text{Mg}^{2+} / \text{Na}^+$ versus $\text{Ca}^{2+} / \text{Na}^+$, (b): $\text{HCO}_3^- / \text{Na}^+$ versus $\text{Ca}^{2+} / \text{Na}^+$.

4.2.3. The Major Weathering and Hydrogeochemical Processes Affecting Groundwater Hydrochemistry

Ions in water mainly originate from atmospheric precipitation, evaporative dissolution of salt from rock weathering and human inputs [31]. The ratio of ions is currently a commonly used method to deduce the source of ions in water. N and K^+ in water mainly originate from meteoric precipitation, weathering and dissolution of silicate minerals and evaporative dissolution of salt minerals. The ratio of the milligram equivalent concentration of Na^+ and Cl^- in atmospheric precipitation is similar to that of Cl^- in seawater, which is 0.86 [23]. The dissolution of rock salt is generally the major source of Na^+ and Cl^- in groundwater in arid/semi-arid areas, and the milligram equivalent ratio of this process is generally approximately one. Figure 6a shows that the majority of shallow groundwater samples from the Jinta Basin were located on the 1:1 line. This illustrates that there are insufficient Cl^- to balance Na^+ , indicating that there are other sources of Na^+ besides rock salt dissolution and atmospheric precipitation. Figure 6e shows that some water samples were located below the 1:1 line, indicating that Na^+ and other cations were required in these samples to balance the anions. These results combined with the results of factor analysis indicated that albite in silicate minerals is likely to be a source of Na^+ .

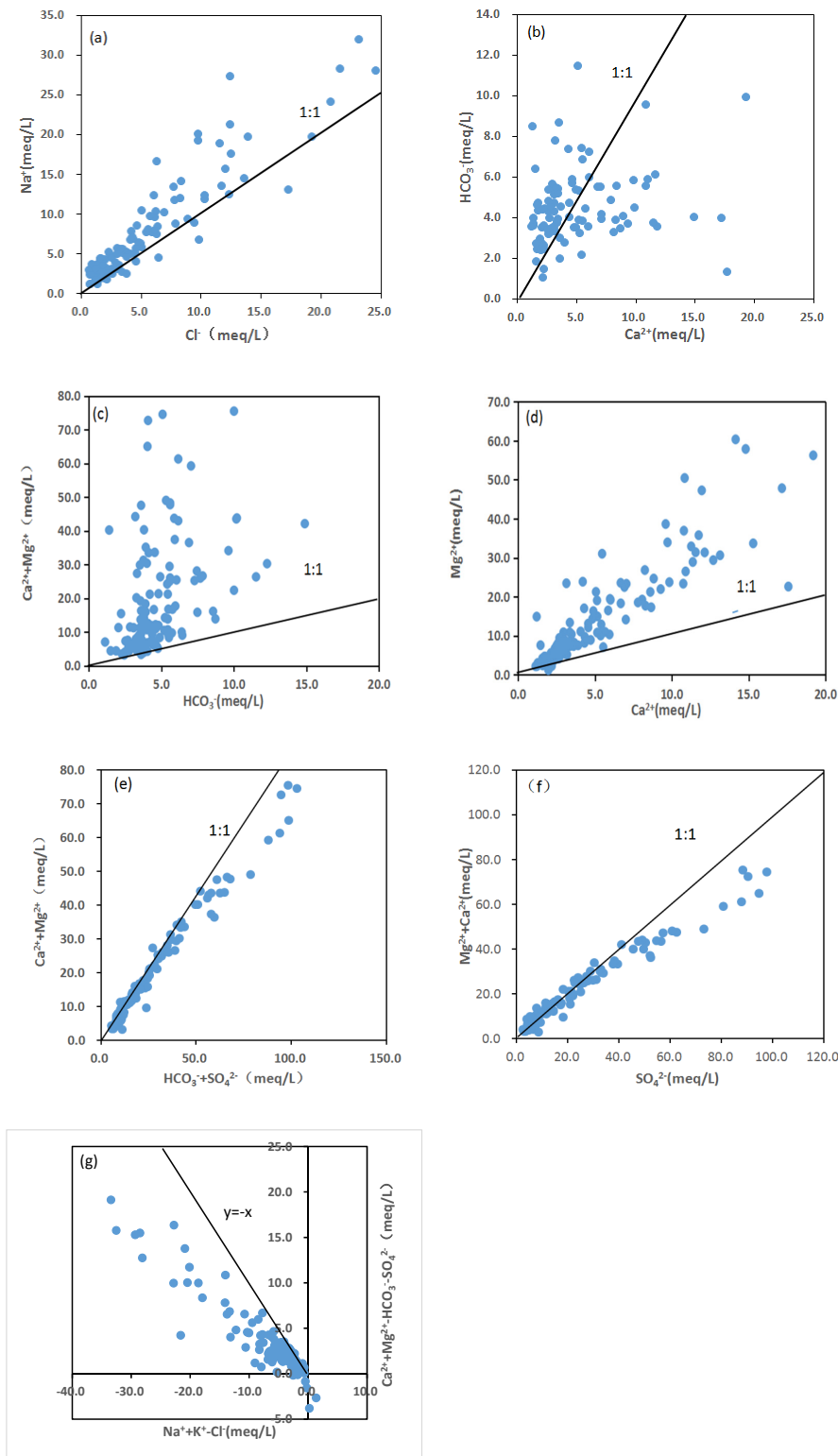
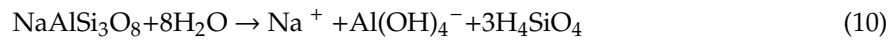


Figure 6. Ratio graphs of ions in groundwater samples collected from the Jinta Basin, China. (a) Na⁺ versus Cl⁻, (b) HCO₃⁻ versus Na⁺, (c) Ca²⁺ + Mg²⁺ versus HCO₃⁻, (d) Mg²⁺ versus Ca²⁺, (e) Ca²⁺ + Mg²⁺ versus HCO₃⁻ + SO₄²⁻, (f) Ca²⁺ + Mg²⁺ versus SO₄²⁻, (g) Ca²⁺ + Mg²⁺ - HCO₃⁻ - SO₄²⁻ versus Na⁺ + K⁺ - Cl⁻

The milligram equivalent concentration ratios of Mg^{2+} , Ca^{2+} and HCO_3^- in water can be used to characterize the dissolution of carbonate rocks in groundwater [32]. Figure 6c shows that only a few water samples were located near the 1:1 line, with the majority positioned above the 1:1 line. Combining these results with those shown in Figure 6b,d, it can be concluded that a few carbonate rocks dissolve in some areas of the Jinta Basin. As shown in Table 5, there were strong correlations between Mg^{2+} and Ca^{2+} and between Mg^{2+} and SO_4^{2-} , with correlation coefficients of 0.727 and 0.959, respectively ($p < 0.01$). Figure 6f shows that the majority of points were located near the 1:1 line, indicating that Mg^{2+} , Ca^{2+} and SO_4^{2-} in groundwater in the basin mainly originate from the dissolution of evaporative salts such as $CaSO_4 \cdot 2H_2O$ (gypsum) and $MgSO_4$. The actual field investigation determined that $Na_2SO_4 \cdot 10H_2O$ (mirabilite) is distributed in the basin; therefore, mirabilite may be another source of SO_4^{2-} in the basin.

Ion exchange is a common phenomenon in the groundwater of inland basins in arid regions. The $(Ca^{2+} + Mg^{2+} - HCO_3^- - SO_4^{2-})$ and $(Na^+ + K^+ - Cl^-)$ ratio methods were used to determine whether ion exchange occurs in the study area. Figure 6g shows that the distribution of most points deviated from $y = -x$. Under no ion exchanges, the distribution of points would fall on the $y = -x$ line; therefore, the effect of ion exchange on shallow groundwater in the study area was minor.

4.3. Groundwater Quality Assessment

4.3.1. Evaluation of Groundwater Samples According to Drinking Water Standards

The calculated WQI values ranged between 45.46–728.71. The WQI classification standard indicated that among the 123 groundwater samples, four showed excellent water quality, 45 showed good water quality, 30 showed general water quality, 19 showed poor water quality and 25 were unsuitable for drinking (Table 6). Figure 7 shows the spatial distribution of the drinking water grades of samples, where it is evident that groundwater samples from the Mazong mountain area were not suitable for drinking, which may be related to their high SO_4^{2-} and Mg^{2+} contents. There was an improvement in the drinking water quality of samples in the western and eastern parts of the basin, whereas those in the middle of the densely populated basin were generally of poor water quality.

Table 6. Classification of groundwater samples collected from the Jinta Basin, China according to calculated parameters standards.

Parameters	Range	Water Class	Number of Samples	Percentage of Samples (%)
SAR	0–9.99	Excellent	123	100
	10–17.99	Good	0	0
	18–26	Doubtful	0	0
	>26	Unsuitable	0	0
Na%	<20	Excellent	0	0
	20–39.99	Good	52	42.28
	40–59.99	Permissible	61	49.59
	60–80	Doubtful	9	7.32
	>80	Unsuitable	1	0.81
KR	<1	Suitable	119	96.75
	1–2	Marginally suitable	4	3.25
	>2	Unsuitable	0	0
PI	<80	Good	122	99.19
	80–100	Moderate	1	0.81
	100–120	Poor	0	0

Abbreviations: SAR: sodium adsorption ratio; Na%: sodium percentage; KR: Kelly's ratio; PI: permeability index.

4.3.2. Evaluation of Groundwater Samples According to Agricultural Irrigation Water Standards

A large proportion of the study area consists of agricultural land, and the majority of irrigation water used in the study area originates from groundwater. The sodium adsorption ratio (SAR),

sodium percentage (Na%), Kelly’s ratio (KR) and permeability index (PI) were calculated to determine the suitability of groundwater for agriculture irrigation (Table 6).

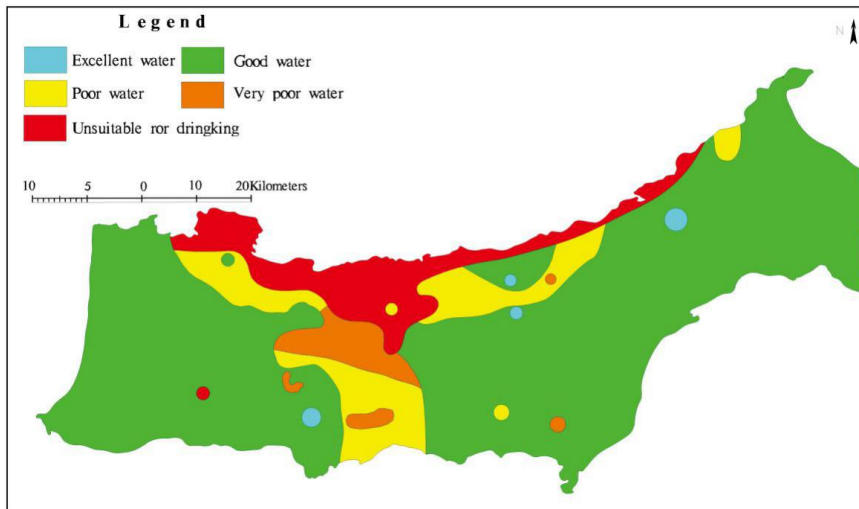


Figure 7. A map showing the suitability of groundwater for drinking within the Jinta Basin, China as according to the water quality index (WQI).

Sodium Adsorption Ratio (SAR)

SAR values of groundwater samples in study area ranged from 0.64 to 9.93. According to the SAR classification, all of the samples in study area fall within the excellent class and were therefore suitable for use in agricultural irrigation (Table 6).

Sodium Percentage (Na%)

Na% values ranged from 23.38 to 84.52. According to water classification based on Na%, 52 groundwater samples in the study area fell within the good category, 61 samples fell into the permissible category and only one sample was deemed to fall in the unsuitable category (Table 6). Figure 8 shows the spatial distribution of Na% in the study basin, where it is evident that irrigation water in the western part of the basin was rated as good, the irrigation water in the eastern part of the basin was rated as permissible and only water samples in the central and northern parts of the basin were rated as doubtful.

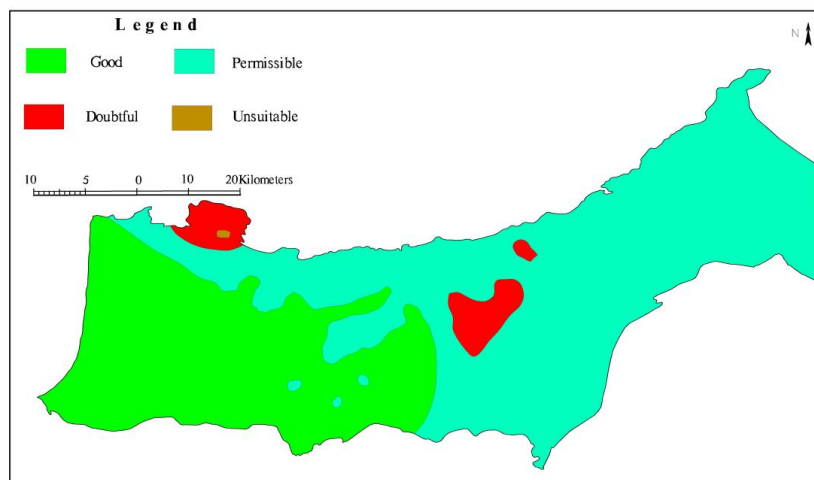


Figure 8. A map showing the suitability of groundwater for agricultural irrigation within the Jinta Basin, China as according to the sodium percentage (Na%).

Kelly's Ratio (KR)

KR values ranged from 0.16 to 1.73. From Table 6, it can be seen that 119 groundwater samples in the study area fell into the suitable category and four samples fell within the marginally suitable category.

Permeability Index (PI)

PI values ranged from 24.33 to 89.75. According to water classification based on PI, 122 groundwater samples in study area fall in the good category whereas only one sample fell in the moderate category (Table 6).

These results showed that the groundwater of the Jinta Basin is suitable for agricultural irrigation.

5. Conclusions

The major cations in shallow groundwater of the Jinta Basin were Na^+ and Mg^{2+} , accounting for more than 77% of the total cations. The major anions were SO_4^{2-} and HCO_3^- , accounting for more than 83% of the total anions. pH of groundwater samples ranged from 7.23 to 8.91, with an average of 7.89. Groundwater samples were therefore generally weakly alkaline. TDS ranged between 328.4–11,513.00 with a mean of 1816.68, and gradually increased along the direction of groundwater runoff.

The major factors controlling the evolution of groundwater chemical types in the Jinta Basin were identified as rock weathering and evaporative crystallization. Chemical components in groundwater mainly originated from the dissolution of silicate rock and evaporate salt, whereas the dissolution of carbonate had little influence on groundwater hydrochemistry. Na^+ and K^+ in the groundwater mainly originated from the dissolution of silicate rocks, such as albite and potassium feldspar, whereas SO_4^{2-} , Ca^{2+} and Mg^{2+} mainly originated from the dissolution of sulphate minerals such as gypsum and mirabilite. The sources of HCO_3^- are complex. Carbonate and silicate rocks are common in aquifers, and their dissolution is one of the main sources of HCO_3^- . Factor analysis showed that human activities also had a great impact on the content of HCO_3^- . The effect of cation exchange on groundwater hydrochemistry was found to be minor.

The water quality index (WQI) was used to determine the suitability of groundwater as drinking water and agricultural irrigation water. The results for drinking water suitability showed that 3.25% of groundwater samples were classified as excellent, 36.59% were found to be good, 24.39% were poor, 15.45% were very poor and 20.32% were unsuitable. SAR, PI, Kr and Na% were used to determine the suitability of groundwater in the basin for use as agricultural irrigation water. SAR classified all water samples as excellent. PI indicated that all groundwater samples except for one were classified as good. The KR classified four groundwater samples as marginally suitable, whereas the remaining 122 groundwater samples were classified as good. The Na% index classified 42.28% groundwater samples as good, 49.59% as permissible, 7.32% as doubtful and only 0.81% as unsuitable. In general, the majority of groundwater in the study area was found to be suitable for use in agricultural irrigation.

Author Contributions: Conceptualization, Z.G., J.F. and J.L.; Methodology, Z.G., J.L. and J.F.; Formal Analysis, Z.G., J.L., F.L., H.S., J.F. and M.H.; Writing-Original Draft Preparation, Z.G., J.L., J.F. and M.H.; Writing-Review & Editing, Z.G., J.L. and J.F.; Resources, X.W. and Y.A.; Project Administration, Z.G., F.L. and H.S.; All authors have read and agreed to the published version of the manuscript.

Funding: This work was supported by Centre for Hydrogeology and Environmental Geology Survey, China Geological Survey. Funded projects are "A 1:50,000 hydrogeological survey of the Heihe River Basin in the Hexi Corridor (DD20160292)" and "Major research project of the national natural science foundation of China: observation and mechanism research on the mutual transformation of surface water and groundwater in Heihe River Basin (91025019)".

Conflicts of Interest: The authors declare no conflict of interest.

References

1. Todd, D.K. *Groundwater Hydrology*, 2nd ed.; Wiley: Hoboken, NJ, USA, 1980.
2. Fetter, C.W. *Applied Hydrogeology*, 3rd ed.; Macmillan College Publication: New York, NY, USA, 1994.

3. Srinivas, Y.; Oliver, D.H.; Raj, A.S.; Chandrasekar, N. Quality assessment and hydrogeochemical characteristics of groundwater in Agastheeswaram taluk, Kanyakumari district, Tamil Nadu, India. *Chin. J. Geochem.* **2014**, *33*, 221–235. [[CrossRef](#)]
4. Wang, S.; Guo, H.Y.; Hu, L.L.; Wang, B. The Relationship between Hydrological Characteristics of Jinta Heihe River Basin and Precipitation. *Hubei Agric. Sci.* **2017**, *56*, 3863–3869.
5. Lu, A.X.; Chen, X.Z.; Wang, J.; Wang, L.H.; Wu, L.Z. Monitoring the Ecology and Environment in the Middle Reaches of the Heihe River Using Remote Sensing. *J. Glaciol. Geocryol.* **2002**, *24*, 73–78.
6. Cui, Z.J.; Xu, Y.Q.; Gao, J.H.; Sun, P.; Gong, J. Land use change and its ecosystem service value evaluation in oasia of Jiuquan-Jinta basin. *Bull. Soil Water Conserv.* **2014**, *34*, 252–257, 272.
7. Li, S. Study on Water Resources Carrying Capacity and Regulation Model in Jinta Basin. Master's Thesis, Lanzhou University, Lanzhou, China, 2017.
8. Ma, L.T. Water Chemistry Characteristics of Groundwater in Heihe River Basin. Master's Thesis, Northwest University, Xi'an, China, 2019.
9. Chen, J. Hydrochemical Characteristics and Its Evolution Modeling of Groundwater in Jinta Basin, Gansu. Master's Thesis, Lanzhou University, Lanzhou, China, 2019.
10. Papazotos, P.; Koumantakis, I.; Vasileiou, E. Hydrogeochemical assessment and suitability of groundwater in a typical Mediterranean coastal area: A case study of the Marathon basin, NE Attica, Greece. *HydroResearch* **2019**, *2*, 49–59. [[CrossRef](#)]
11. Alexakis, D. Meta-Evaluation of Water Quality Indices. Application into Groundwater Resources. *Water* **2020**, *12*, 1890. [[CrossRef](#)]
12. Gu, X.M.; Xiao, Y.; Yin, S.Y.; Hao, Q.C.; Liu, H.L.; Hao, Z.Y.; Meng, G.P.; Pei, Q.M.; Yan, H.J. Hydrogeochemical Characterization and Quality Assessment of Groundwater in a Long-Term Reclaimed Water Irrigation Area, North China Plain. *Water* **2018**, *10*, 1209. [[CrossRef](#)]
13. Abbasnia, A.; Yousefi, N.; Mahvi, A.H.; Nabizadeh, R.; Radfard, M.; Yousefi, M.; Alimohammadi, M. Evaluation of groundwater quality using water quality index and its suitability for assessing water for drinking and irrigation purposes: Case study of Sistan and Baluchistan province (Iran). *Hum. Ecol. Risk Assess.* **2019**, *25*, 988–1005. [[CrossRef](#)]
14. Karim, A.; Cruz, M.G.; Hernandez, E.A.; Uddameri, V. A GIS-Based Fit for the Purpose Assessment of Brackish Groundwater Formations as an Alternative to Freshwater Aquifers. *Water* **2020**, *12*, 2299. [[CrossRef](#)]
15. Chitsazan, M.; Aghazadeh, N.; Mirzaee, Y.; Golestan, Y. Hydrochemical characteristics and the impact of anthropogenic activity on groundwater quality in suburban area of Urmia city, Iran. *Environ. Dev. Sustain.* **2019**, *21*, 331–351. [[CrossRef](#)]
16. Abhisheka, V.R.; Kumar, R.B.B. Groundwater quality assessment for domestic and irrigational suitability in Kallada River Basin, South Kerala, India. *Nat. Environ. Pollut. Technol.* **2018**, *17*, 153–159.
17. Shahab, A.; Qi, S.H.; Zaheer, M.; Rashid, A.; Talib, M.A.; Ashraf, U. Hydrochemical characteristics and water quality assessment for drinking and agricultural purposes in District Jacobabad, Lower Indus Plain, Pakistan. *Int. J. Agric. Biol. Eng.* **2018**, *11*, 115–121. [[CrossRef](#)]
18. Sunitha, V.; Reddy, Y.S. Hydrogeochemical evaluation of groundwater in and around Lakkireddipalli and Ramapuram, Y.S.R District, Andhra Pradesh, India. *HydroResearch* **2019**, *2*, 85–96. [[CrossRef](#)]
19. Brindha, K.; Kavitha, R. Hydrochemical assessment of surface water and groundwater quality along Uyyakondan channel, south India. *Environ. Earth Sci.* **2015**, *73*, 5383–5393. [[CrossRef](#)]
20. Kelley, W.P.; Brown, S.M.; Liebig, G.F.J. Chemical effects of saline irrigation water on soils. *Soil Sci.* **1940**, *49*, 95–108. [[CrossRef](#)]
21. Doneen, L.D. Notes on water quality in agriculture. In *Water Science and Engineering Paper 4001*; Department of Water Sciences and Engineering, University of California: Oakland, CA, USA, 1964.
22. Koffi, K.V.; Obuobie, E.; Banning, A.; Wohnlich, S. Hydrochemical characteristics of groundwater and surface water for domestic and irrigation purposes in Veve catchment, Northern Ghana. *Environ. Earth Sci.* **2017**, *76*, 185. [[CrossRef](#)]
23. Yang, Q.C.; Li, Z.J.; Ma, H.Y.; Wang, L.C.; Martin, J.D. Identification of the hydrogeochemical processes and assessment of groundwater quality using classic integrated geochemical methods in the Southeastern part of Ordos basin, China. *Environ. Pollut.* **2016**, *218*, 879–888. [[CrossRef](#)]
24. Zhou, P.P.; Wang, Z.M.; Zhang, J.Y.; Yang, Z.X.; Li, X.L. Study on the hydrochemical characteristics of groundwater along the Taklimakan Desert Highway. *Environ. Earth Sci.* **2016**, *75*, 1378. [[CrossRef](#)]

25. Paul, R.; Brindha, K.; Gowrisankar, G.; Tan, M.L.; Singh, M.K. Identification of hydrogeochemical processes controlling groundwater quality in Tripura, Northeast India using evaluation indices, GIS, and multivariate statistical methods. *Environ. Earth Sci.* **2019**, *78*, 470. [[CrossRef](#)]
26. Brindha, K.; Pavelic, P.; Sotoukee, T.; Douangsavanh, S.; Elango, L. Geochemical Characteristics and Groundwater Quality in the Vientiane Plain, Laos. *Expo. Health* **2016**, *9*, 89–104. [[CrossRef](#)]
27. Liu, J.T.; Gao, Z.J.; Wang, Z.Y.; Xu, X.Y.; Su, Q.; Wang, S.; Qu, W.L.; Xing, T.J. Hydrogeochemical processes and suitability assessment of groundwater in the Jiaodong Peninsula, China. *Environ. Monit. Assess.* **2020**, *192*, 384. [[CrossRef](#)] [[PubMed](#)]
28. Piper, A.M. A graphic procedure in the geochemical interpretation of water-analysis. *Trans. Am. Geophys. Union* **1944**, *25*, 914–923. [[CrossRef](#)]
29. Gibbs, R.J. Mechanisms controlling world water chemistry. *Science* **1970**, *170*, 1088–1099. [[CrossRef](#)] [[PubMed](#)]
30. Gaillardet, J.; Dupré, B.; Louvat, P.; Allègre, C.J. Global silicate weathering and CO₂ consumption rates deduced from the chemistry of large rivers. *Chem. Geol.* **1999**, *159*, 3–30. [[CrossRef](#)]
31. Liu, J.T.; Gao, Z.J.; Wang, M.; Li, Y.Z.; Shi, M.J.; Zhang, H.Y.; Ma, Y.Y. Hydrochemical characteristics and possible controls in the groundwater of the Yarlung Zangbo River Valley, China. *Environ. Earth Sci.* **2019**, *78*. [[CrossRef](#)]
32. Nematollahi, M.J.; Ebrahimi, P.; Razmara, M.; Ghasemi, A. Hydrogeochemical investigations and groundwater quality assessment of Torbat-Zaveh plain, Khorasan Razavi, Iran. *Environ. Monit. Assess.* **2016**, *2*, 188. [[CrossRef](#)]



© 2020 by the authors. Licensee MDPI, Basel, Switzerland. This article is an open access article distributed under the terms and conditions of the Creative Commons Attribution (CC BY) license (<http://creativecommons.org/licenses/by/4.0/>).